

# A FIXATION-BASED 360° BENCHMARK DATASET FOR SALIENT OBJECT DETECTION

Yi Zhang<sup>†</sup>, Lu Zhang<sup>†</sup>, Wassim Hamidouche<sup>†</sup>, Olivier Deforges<sup>†</sup>

<sup>†</sup> IETR INSA Rennes, France

## ABSTRACT

Fixation prediction (FP) in panoramic contents has been widely investigated along with the booming trend of virtual reality (VR) applications. However, another issue within the field of visual saliency, salient object detection (SOD), has been seldom explored in 360° (or omnidirectional) images due to the lack of datasets representative of real scenes with pixel-level annotations. Toward this end, we collect 107 equirectangular panoramas with challenging scenes and multiple object classes. Based on the consistency between FP and explicit saliency judgements, we further manually annotate 1,165 salient objects over the collected images with precise masks under the guidance of real human eye fixation maps. Six state-of-the-art SOD models are then benchmarked on the proposed fixation-based 360° image dataset (**F-360iSOD**), by applying a multiple cubic projection-based fine-tuning method. Experimental results show a limitation of the current methods when used for SOD in panoramic images, which indicates the proposed dataset is challenging. Key issues for 360° SOD is also discussed. The proposed dataset is available at <https://github.com/Panorama-Bill/F-360iSOD>.

**Index Terms**— VR, salient object detection, 360-degree image dataset, equirectangular panorama, benchmark

## 1. INTRODUCTION

The panoramic image, or 360° (omnidirectional) image, which captures the content on the whole 360×180° viewing range surrounding a viewer, plays an import role in virtual reality (VR) applications and distinguishes itself from traditional 2-dimensional (2D) image which covers only one specific plane. Recently, commercial Head-Mounted Displays (HMDs) are developed to provide observers an immersive even interactive experience by allowing them to freely rotate their head and thus focusing on desired scenes and objects. Considering the fact that some salient parts of the 360° image attract more human attentions than others [1], visual saliency prediction in panoramas becomes one of the focused issues within the field of computer vision and is considered as a key to study human observation behavior in virtual environments. The fixation prediction (FP) and salient object detection (SOD) are both closely related to the concept of visual saliency. Thanks to the accessibility of HMDs and eye

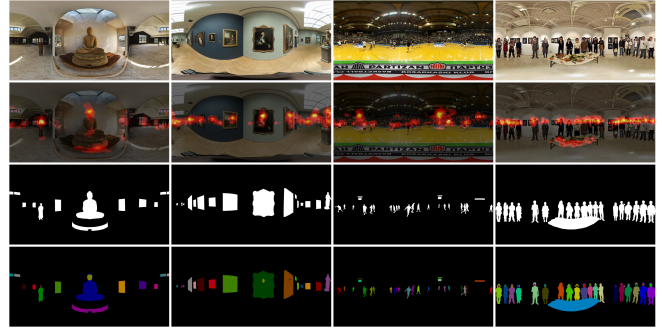


**Fig. 1:** Representative samples of the proposed fixation-based 360° image dataset (**F-360iSOD**). The first row: four panoramic images presented in the equirectangular format; the second row: images overlaid with thresholded fixation maps; the third row: object-level ground-truths; the fourth row: instance-level ground-truths.

trackers, image [2] and video (e.g., [3–5]) datasets have been constructed for the deep learning-based FP in panoramic content. However, to the best of knowledge, [6] is the only study for SOD in 360° scenarios, which does not use the fixations as a guidance for the salient object annotation.

As shown in Fig. 1, 360° images tend to have richer scenes and much more foreground objects compared to flat-2D images from traditional SOD datasets (e.g., [7–12]). Therefore, it is more challenging to differentiate the salient objects from the non-salient ones in panoramas. Preserving 360° images with a few obvious foreground objects while discarding those ambiguous ones may bring selection bias to the dataset, thus being inefficient for exploring the real human attention behavior as viewing panoramic content. Based on the strong correlation between FP and explicit human judgements [13], and the successfully established fixation-based 2D SOD datasets [13–15], we argue that the salient objects in panoramas can also be manually annotated with the assistance of fixations, thus representing the real-world daily scenes. The main contributions of this paper are: **1)** a fixation-based 360° image dataset (**F-360iSOD**) with both the object-/instance-level pixel-wise annotations is proposed; **2)** six newly proposed state-of-the-art 2D SOD models [16–21] are benchmarked by five widely used SOD metrics [22–26] on the proposed dataset in a cross-testing manner, with a multiple cubic projection-based fine-tuning strategy [27]; **3)** key issues for 360° SOD are discussed.



to manually annotate (by tracing boundaries) the salient objects with both the object-/instance-level masks on the collected equirectangular images, under the guidance of fixation maps convoluted by a Gaussian with a standard deviation empirically set to  $2^\circ$  of visual angle (note that each of the Gaussian-smoothed fixation maps is thresholded with an adaptive saliency value to keep the top one-10th of each self before shown to the annotator). The whole annotation process has been repeated three times to pass the quality check implemented by two other experts, for the final ground-truths. Besides, nine images without any salient object annotations are kept in **F-360iSOD**, to avoid the common bias of 2D SOD datasets (as mentioned in [33]), brought by an assumption that there is at least one salient object in each of the image.

### 3.3. Dataset Statistics

In **F-360iSOD**, each of the salient object belongs to one specific class. Generally, there are 1,165 salient objects from 72 categories, thus reflecting 7 aspects (human, text, vehicle, architecture, artwork, animal and daily stuff) of the real-world common scenes (Fig. 2). The *person* category occupies the largest proportion with a number of instances of 386; other relative large object classes include *painting*, *text*, *building*, *person face* and *car*, with a number of instances of 92, 89, 86, 75 and 72, respectively.

## 4. EXPERIMENTAL RESULTS AND DISCUSSIONS

### 4.1. Dataset Split

The **F-360iSOD** consists of one training set and two testing set, which are denoted as F-360iSOD-train, F-360iSOD-testA and F-360iSOD-testB, respectively. The F-360iSOD-train contains 68 equirectangular images from the Saliency360 [2], while the F-360iSOD-testA collects the remaining 17 (85 in total). Besides, the F-360iSOD-testB is established to enable the cross-testing for SOD models, with 22 images from another panoramic image dataset (Stanford360 [1]).

### 4.2. Projection Methods

By wearing HMDs, people are able to freely rotate their head to make multiple viewports focusing on the attractive regions of the surrounding  $360^\circ$  content. Based on this prior knowledge, we apply cubemap projection (where a  $360^\circ$  image is projected into 6 rectangular patches) to process 68 panoramic images (from F-360iSOD-train) with multiple rotation angles ( $0^\circ$ ,  $30^\circ$ ,  $60^\circ$  both horizontally and vertically [27]). Therefore, we gain 54 ( $6 \times 3 \times 3$ ) patches representative of multiple fields of view for each of the  $360^\circ$  image. 3672 ( $54 \times 68$ ) 2D patches ( $256 \times 256$ ) are therefore generated and used as inputs for the fine-tuning of 2D SOD models.

### 4.3. Evaluation Metrics

To measure the agreement between manually labeled ground-truths and model predictions, we adopt five widely used SOD

metrics: F-measure curves [22], weighted  $F_\beta$  measure (Fbw) [23], mean absolute error (MAE) [25], structural measure (S-measure) [24] and enhanced-alignment measure (E-measure) curves [26]. Note that the  $\beta^2$  is set to 0.3 in F-measure and Fbw, aiming to emphasize more on precision as suggested in [22]. F-measure, MAE and Fbw address the pixel-wise errors, while S-measure evaluates the structural similarity between predicted saliency maps and binary ground-truths :

$$S = \alpha \times S_o + (1 - \alpha) \times S_r, \quad (1)$$

where  $S_o$  and  $S_r$  denote the object-/region-aware structure similarities, respectively;  $\alpha$  is empirically set to 0.7 ( $\alpha = 0.5$  in 2D) to attach more importance on object structure, based on the observation that panoramic images are usually dominated by small salient objects distributed over the whole image (e.g., Fig. 1), rather than one or multiple spatially connected foreground objects located at the center of the image. E-measure is a more recently proposed SOD metric which combines both the pixel-/image-level information:

$$Q_{FM} = \frac{1}{W \times H} \sum_{i=1}^W \sum_{j=1}^H \phi_{FM}(x, y), \quad (2)$$

where the  $\phi_{FM}$  means the enhanced alignment matrix; the  $H$  and  $M$  are the height and width of the foreground map.

### 4.4. Benchmarking Results

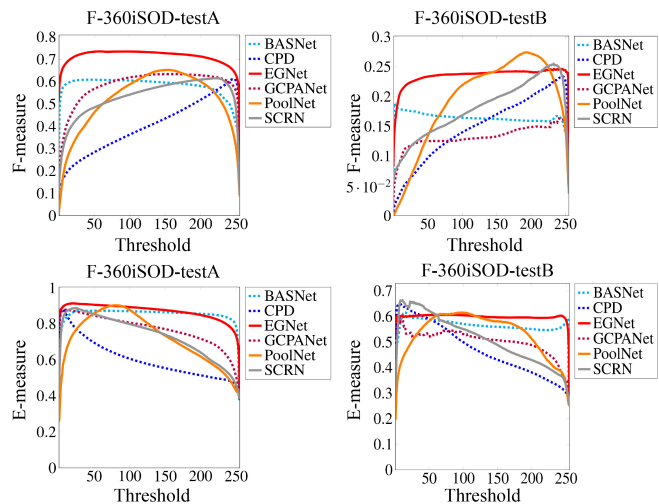


**Fig. 3:** F-measure curves and E-measure curves obtained by six state-of-the-art SOD models on the **F-360iSOD**.

In our study, each of the SOD model is fine-tuned on the F-360iSOD-train with an initial learning rate of one-tenth of the default, and a batch size of 1. The training process will stop as the S-measure value on the F-360iSOD-testA starts to go down. As a result, it takes about 20 epochs for BASNet [16], EGNet [17], CPD [19] and SCRN [20] to converge, while 70 for PoolNet [18] and 15 for GCPANet [21]. The quantitative and qualitative comparison between the six state-of-the-art 2D SOD models on both the F-360iSOD-testA/B are illustrated in Table. 1, Fig. 3 and Fig. 4, respectively.

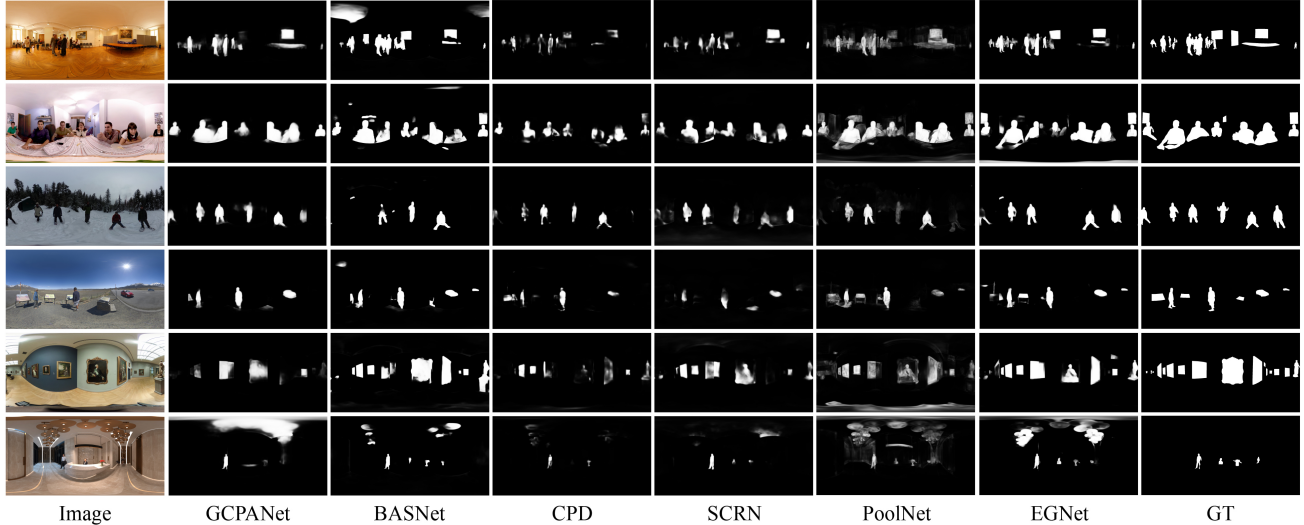


Fig. 4: A qualitative comparison between six state-of-the-art SOD models on F-360iSOD.

Methods	F-360iSOD-testA			F-360iSOD-testB		
	$F_{\beta}^w \uparrow$	$S \uparrow$	$MAE \downarrow$	$F_{\beta}^w \uparrow$	$S \uparrow$	$MAE \downarrow$
SCRN [20]	.551	.809	.050	.124	.708	.034
BASNet [16]	.567	.825	.046	.118	.683	.048
CPD [19]	.521	.763	.052	.129	.695	.032
PoolNet [18]	.500	.834	.068	.136	.716	.058
GCPANet [21]	.630	.822	.045	.106	.693	.039
EGNet [17]	.715	.864	.045	.190	.714	.041

Table 1: A quantitative comparison between six state-of-the-art SOD models on F-360iSOD, where  $F_{\beta}^w$  means Fbw,  $S$  represents S-measure. Note that the top three results of each column are highlighted in red, green and blue, respectively.

#### 4.5. Discussions

**Features of 360° datasets.** All the benchmarking models are constrained to some extent on the proposed F-360iSOD, even though achieving high performances in 2D SOD [16–21]. The limitation is mainly due to the challenges brought by the features of 360° dataset, such as equirectangular projection-induced distortions, small objects and clutter scenes, etc.

**Fixation-based complexity analysis.** Since the panoramic images tend to contain much more scenes and objects than 2D images, the ambiguity of saliency judgements in panoramas should also be considered, which can be quantified by inter observer congruency (IOC) [34] and entropy based on fixation maps (note that the fixation maps are smoothed with a Gaussian with a standard deviation of 1° visual angle, as suggested in [1]). As an image with high IOC and low entropy is usually considered to be simple, the F-360iSOD-testB should be easier to explore when compared with the F-360iSOD-testA (Fig. 5), from a perspective of human judgements.

**Unseen object classes.** All benchmarking models fail on the

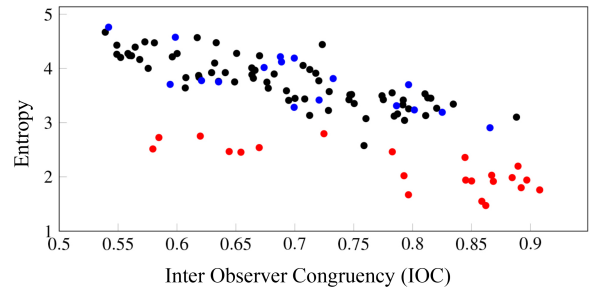


Fig. 5: A fixation-based complexity analysis of the proposed F-360iSOD. The F-360iSOD-train, F-360iSOD-testA/B are annotated in black, blue and red, respectively.

F-360iSOD-testB, mainly due to the presence of unseen object classes in Stanford360 [1], such as sharks, bells, robots, etc. People are capable of recognizing new object categories when provided with high-level descriptions. This strong generalization ability is still absent in current SOD models.

**Instance-level ground-truths.** As far as we know, the proposed F-360iSOD is the first 360° dataset that provides instance-level semantic labels for salient objects. Future SOD models must be able to recognize the individual instances of multiple classes, which is crucial for practical applications, such as image captioning, scene understanding, etc.

## 5. CONCLUSIONS

In this paper, we propose a fixation-based 360° image dataset (F-360iSOD), with precisely annotated salient objects/instances from multiple classes representative of real-world daily scenes. Six recently proposed top-performed SOD methods are fine-tuned and tested on the F-360iSOD. Results show a limit of current 2D models when directly applied to the SOD in panoramas. We believe the F-360iSOD can be used as one of the basic panoramic datasets and thus supporting future 360° SOD model development.

## 6. REFERENCES

- [1] Vincent Sitzmann, Ana Serrano, Amy Pavel, Maneesh Agrawala, Diego Gutierrez, Belen Masia, and Gordon Wetzstein, "Saliency in vr: How do people explore virtual environments?," *IEEE TVCG*, vol. 24, no. 4, pp. 1633–1642, 2018.
- [2] Yashas Rai, Jesús Gutiérrez, and Patrick Le Callet, "A dataset of head and eye movements for 360 degree images," in *MMSys*. ACM, 2017, pp. 205–210.
- [3] Chen Li, Mai Xu, Xinzhe Du, and Zulin Wang, "Bridge the gap between vqa and human behavior on omnidirectional video: A large-scale dataset and a deep learning model," in *ACM MM*, 2018, pp. 932–940.
- [4] Yanyu Xu, Yanbing Dong, Junru Wu, Zhengzhong Sun, Zhiru Shi, Jingyi Yu, and Shenghua Gao, "Gaze prediction in dynamic 360 immersive videos," in *IEEE CVPR*, 2018, pp. 5333–5342.
- [5] Ziheng Zhang, Yanyu Xu, Jingyi Yu, and Shenghua Gao, "Saliency detection in 360 videos," in *ECCV*, 2018, pp. 488–503.
- [6] Jia Li, Jinming Su, Changqun Xia, and Yonghong Tian, "Distortion-adaptive salient object detection in 360 omnidirectional images," *IEEE JSTSP*, 2019.
- [7] Qiong Yan, Li Xu, Jianping Shi, and Jiaya Jia, "Hierarchical saliency detection," in *IEEE CVPR*, 2013, pp. 1155–1162.
- [8] Vida Movahedi and James H Elder, "Design and perceptual validation of performance measures for salient object segmentation," in *CVPRw*. IEEE, 2010, pp. 49–56.
- [9] Yin Li, Xiaodi Hou, Christof Koch, James M Rehg, and Alan L Yuille, "The secrets of salient object segmentation," in *IEEE CVPR*, 2014, pp. 280–287.
- [10] Guanbin Li and Yizhou Yu, "Visual saliency based on multi-scale deep features," in *IEEE CVPR*, 2015, pp. 5455–5463.
- [11] Lijun Wang, Huchuan Lu, Yifan Wang, Mengyang Feng, Dong Wang, Baocai Yin, and Xiang Ruan, "Learning to detect salient objects with image-level supervision," in *IEEE CVPR*, 2017, pp. 136–145.
- [12] Chuan Yang, Lihe Zhang, Huchuan Lu, Xiang Ruan, and Ming-Hsuan Yang, "Saliency detection via graph-based manifold ranking," in *IEEE CVPR*, 2013, pp. 3166–3173.
- [13] Ali Borji, "What is a salient object? a dataset and a baseline model for salient object detection," *IEEE TIP*, vol. 24, no. 2, pp. 742–756, 2014.
- [14] Jia Li, Changqun Xia, and Xiaowu Chen, "A benchmark dataset and saliency-guided stacked autoencoders for video-based salient object detection," *IEEE TIP*, vol. 27, no. 1, pp. 349–364, 2017.
- [15] Deng-Ping Fan, Wenguan Wang, Ming-Ming Cheng, and Jianbing Shen, "Shifting more attention to video salient object detection," in *IEEE CVPR*, 2019, pp. 8554–8564.
- [16] Xuebin Qin, Zichen Zhang, Chenyang Huang, Chao Gao, Masood Dehghan, and Martin Jagersand, "Basnet: Boundary-aware salient object detection," in *IEEE CVPR*, 2019, pp. 7479–7489.
- [17] Jia-Xing Zhao, Jiang-Jiang Liu, Deng-Ping Fan, Yang Cao, Jufeng Yang, and Ming-Ming Cheng, "Egnet: Edge guidance network for salient object detection," in *IEEE ICCV*, 2019, pp. 8779–8788.
- [18] Jiang-Jiang Liu, Qibin Hou, Ming-Ming Cheng, Jiashi Feng, and Jianmin Jiang, "A simple pooling-based design for real-time salient object detection," in *IEEE CVPR*, 2019.
- [19] Zhe Wu, Li Su, and Qingming Huang, "Cascaded partial decoder for fast and accurate salient object detection," in *IEEE CVPR*, 2019, pp. 3907–3916.
- [20] Zhe Wu, Li Su, and Qingming Huang, "Stacked cross refinement network for edge-aware salient object detection," in *IEEE ICCV*, 2019, pp. 7264–7273.
- [21] Chen Zuyao, Xu Qianqian, Cong Runmin, and Huang Qingming, "Global context-aware progressive aggregation network for salient object detection," in *AAAI*, 2020.
- [22] Radhakrishna Achanta, Sheila Hemami, Francisco Estrada, and Sabine Süsstrunk, "Frequency-tuned salient region detection," in *IEEE CVPR*, 2009, pp. 1597–1604.
- [23] Ran Margolin, Lihi Zelnik-Manor, and Ayellet Tal, "How to evaluate foreground maps?," in *IEEE CVPR*, 2014, pp. 248–255.
- [24] Deng-Ping Fan, Ming-Ming Cheng, Yun Liu, Tao Li, and Ali Borji, "Structure-measure: A new way to evaluate foreground maps," in *IEEE ICCV*, 2017, pp. 4548–4557.
- [25] Federico Perazzi, Philipp Krähenbühl, Yael Pritch, and Alexander Hornung, "Saliency filters: Contrast based filtering for salient region detection," in *IEEE CVPR*, 2012, pp. 733–740.
- [26] Deng-Ping Fan, Cheng Gong, Yang Cao, Bo Ren, Ming-Ming Cheng, and Ali Borji, "Enhanced-alignment measure for binary foreground map evaluation," *IJCAI*, pp. 698–704, 2018.
- [27] Fang-Yi Chao, Lu Zhang, Wassim Hamidouche, and Olivier Deforges, "Salgan360: visual saliency prediction on 360 degree images with generative adversarial networks," in *ICMEw*. IEEE, 2018, pp. 01–04.
- [28] Deng-Ping Fan, Ming-Ming Cheng, Jiang-Jiang Liu, Shang-Hua Gao, Qibin Hou, and Ali Borji, "Salient objects in clutter: Bringing salient object detection to the foreground," in *ECCV*, 2018, pp. 186–202.
- [29] Deng-Ping Fan, Zheng Lin, Jia-Xing Zhao, Yun Liu, Zhao Zhang, Qibin Hou, Menglong Zhu, and Ming-Ming Cheng, "Rethinking rgb-d salient object detection: Models, datasets, and large-scale benchmarks," *arXiv preprint arXiv:1907.06781*, 2019.
- [30] Xavier Corbillon, Francesca De Simone, and Gwendal Simon, "360-degree video head movement dataset," in *MMSys*. ACM, 2017, pp. 199–204.
- [31] Mai Xu, Chen Li, Yufan Liu, Xin Deng, and Jiaxin Lu, "A subjective visual quality assessment method of panoramic videos," in *ICME*. IEEE, 2017, pp. 517–522.
- [32] Mai Xu, Yuhang Song, Jianyi Wang, MingLang Qiao, Liangyu Huo, and Zulin Wang, "Predicting head movement in panoramic video: A deep reinforcement learning approach," *IEEE TPAMI*, 2018.
- [33] Yi Zhang, Lu Zhang, Wassim Hamidouche, and Olivier Deforges, "Key issues for the construction of salient object datasets with large-scale annotation," in *IEEE MIPR*, 2020.
- [34] Olivier Le Meur, Thierry Baccino, and Aline Roumy, "Prediction of the inter-observer visual congruency (iovc) and application to image ranking," in *ACM MM*, 2011, pp. 373–382.